ELSEVIER

Marine Geology 197 (2003) 95–116

MARINE GEOLOGY
INTERNATIONAL JOURNAL OF MARINE GEOLOGY, GEOCHEMISTRY AND GEOPHYSICS

www.elsevier.com/locate/margeo

A morphological model of the beach profile integrating wave and tidal influences

A.M. Bernabeu [a,*], R. Medina [b], C. Vidal [b]

[a] *Departamento de Geociencias Marinas y O.T., Universidad de Vigo, 36200 Vigo, Spain*
[b] *Ocean and Coastal Research Group, Departamento de Ciencias y Técnicas del Agua y del M. A., Universidad de Cantabria, 39005 Santander, Spain*

Received 26 February 2002; accepted 6 March 2003

Abstract

Meso- and macrotidal beaches constitute a significant proportion of the world's beaches. However, by far, they have been less studied and understood than tideless beaches. Even though in recent times several local studies have addressed this problem, few attempts to model tidal beaches exist. A morphological model capable of predicting the beach profile behaviour under different wave and tide conditions is proposed. It is based on the concept of the two-section equilibrium beach profile, and has been validated with field and laboratory data. This is achieved by means of two parameters: the modal tidal range and the dimensionless fall velocity. Tide is considered a local variable whose principal effect is the lengthening of the intertidal profile. The greater the tidal range, the wider the intertidal profile, here defined as the surf profile. The dimensionless fall velocity defines the transition from dissipative to reflective situations in beaches of any given tidal range. Wave height is the controlling parameter in seasonal beach changes: as the wave height decreases, the beach profile changes from erosive to accumulative. These morphological changes in the surf and shoaling sections of the profile occur in the opposite direction. Whilst in the surf profile the slope of the upper part of this section becomes steeper and the concavity of whole section increases; in the shoaling profile, the upper part flattens resulting in a less concave section. In this transition, the slope break between surf and shoaling profiles, here defined as the discontinuity point, becomes smoother and difficult to identify. The main morphological parameter of the model, x_o, describes the length of the surf profile. This parameter is capable of expressing slightly different variability in micro-, meso- and macrotidal beaches. In microtidal beaches, the length of the surf profile decreases proportionally to the dimensionless fall velocity; in meso- and macrotidal beaches x_o decreases from the dissipative to the intermediate state, but increases from intermediate to reflective. This results from the flattening of the lower part of the surf profile in the reflective case, where a small change in tidal range generates a high stretching of the surf profile. This beach morphological model is presented as a framework to understand the first-order behaviour of beaches under the action of waves and tides. This becomes a useful and easy-to-apply tool in coastal management and prediction of equilibrium beach profile under diverse conditions.

Keywords: equilibrium beach profile; modal tidal range; dimensionless fall velocity; morphological model; Spain

* Corresponding author. Fax: +34-986-81-25-56. *E-mail address:* bernabeu@uvigo.es (A.M. Bernabeu).

0025-3227/03/$ – see front matter © 2003 Elsevier Science B.V. All rights reserved.
doi:10.1016/S0025-3227(03)00087-2

1. Introduction

The morphology of a beach is mainly controlled by wave climate, tide and sediment characteristics (Bagnold, 1940; Bascom, 1951; Johnson, 1956; King, 1972; Duncan, 1964; Strahler, 1966; Clarke et al., 1984; Eliot and Clarke, 1988). Davis and Hayes (1984) suggested the concept of relative (RTR = TR/H) rather than absolute tide range. They pointed out that beach morphodynamics is a response to the interaction of wave height and tidal range. However, most beach morphodynamical-state prediction-oriented models are exclusively developed as a function of wave and sediment parameters (Sonu, 1973; Sunamura, 1989; Lippman and Holman, 1990). The widely used classification proposed by Wright and Short (1984) attempts to integrate the depositional forms and hydrodynamic processes that influence the beach. This model identifies six basic beach states comprising two extreme wave energy states defined as dissipative (high) and reflective (low), and four intermediate states. Whilst the extreme states can be described simply in terms of the beach profile slope (flat and steep, respectively), the intermediate states incorporate three-dimensional morphological characteristics, accounting for more complex circulation patterns and bar–trough systems.

Each morphodynamical state is related to specific incident waves and sedimentary conditions, using the dimensionless fall velocity parameter (Dean, 1973; Dalrymple and Thompson, 1977):

$$\Omega = \frac{H_b}{wT} \quad (1)$$

where H_b is the modal breaker wave height, T is the period and w is the sediment fall velocity. The morphodynamical variability of a beach is determined by the range of sediment and waves change. This morphodynamical model is based on data measured on microtidal beaches from Australia. Consequently, the effect of large daily sea level changes associated with tides is not included. The first attempt to order the macrotidal systems was developed by Carter (1988). He observed five types of beaches as a function of their energy level, using a significant collection of data published at that time. Short (1991) tried to develop a morphodynamical model including the tidal effect, based on previously published data and his own measurements. Taking into account the topographic gradient and the relative sea-swell energy, he identified three classes: two beach states and one transitional situation. This assemblage of beach types was based mainly on the breaker wave height (H_b) and, consequently, each group encompassed a wide range of sedimentary characteristics, tide and beach morphologies. The morphodynamical classifications of Carter (1988) and Short (1991) indirectly account for the tide, but they do not study or subsequently explain the effect of the tide on the beach morphodynamics.

Following the work of Wright and Short (1984) and Short (1991), Masselink and Short (1993) proposed a beach evolution model that accounted for the tidal effect. Their model is defined as a function of two dimensionless parameters: the dimensionless fall velocity Ω (Wright and Short, 1984), which discriminates different states; and the relative tide range (RTR), given by the ratio of tide range to breaker height (Davis and Hayes, 1984). This conceptual model includes the tidal influence as a passive process whose main consequence is to expose and submerge the beach profile during a tidal cycle. This changes the time that the swash, surf zone and the shoaling processes act on the beach profile and subsequently their relative importance, decreasing the sediment transport rate and slowing down the morphological changes.

Masselink and Short (1993), fully aware of the limitations of their approach, called for further work to improve the knowledge of the macrotidal beach morphodynamics, proposing their conceptual model as a starting point for future studies. Since then, numerous local studies have dealt with different aspects of meso- and macrotidal beaches (Horn, 1993; Levoy et al., 1994; Masselink and Hegge, 1995; Foote et al., 1998; Benavente et al., 2000; Levoy et al., 2001; Kroon and Masselink, 2002) although very few have attempted to model them (Masselink, 1993).

Joining the effort to study in depth the meso- and macrotidal beaches, this work proposes a

model of the beach profile morphology that fully includes and analyses the tidal effect. The model is based on the concept of the equilibrium beach profile (Fenneman, 1902; Brunn, 1954; Vellinga, 1983; Dean, 1977, 1987, 1991; Larson, 1991; Bodge, 1992; Komar and McDougal, 1994). The two-section profile (surf and shoaling zones) considered here is based on similar developments previously approached by others authors (Everts, 1978; Bowen, 1980; Inman et al., 1993; Larson et al., 1999).

Our approach is threefold. Firstly, we have selected a number of beaches of which the profiles (including their subtidal part), sediment characteristics, wave climate and tide range have been measured and are known in great detail. This data set comprises a wide variety of conditions on which the empirical validation of the proposed time-evolution model can be based.

Secondly, we introduce a brief explanation of the two-section equilibrium beach profile model (2S-EBP) and the tidal influence on the beach profile laying the theoretical foundations of the proposed morphological model. These foundations have been proposed previously and validated by Bernabeu (1999) and Bernabeu et al. (in press). The predictive capabilities of the model are also discussed against an independent data set. The profile morphology was approximated for different times of the year considering their corresponding wave conditions and sediment characteristics.

Finally, the waves-and-tide integrated model of the beach profile is fully developed. The model provides a formulation that predicts the beach profile shape, based on the dimensionless fall velocity and modal tidal range. The model assumes that the beach has had enough time to adapt to each wave condition. Further, this general 2-D model not only integrates the established understanding compiled in the morphodynamical models of Wright and Short (1984) for tideless beaches and Masselink and Short (1993) for beaches with significant tides, but provides a validation scheme based on measured data.

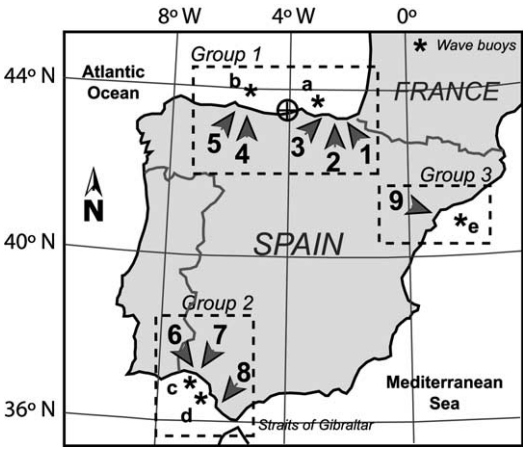

Fig. 1. Location of the studied beaches along the Spanish coast: (1) Zumaia Beach, (2) Zarautz Beach, (3) Bakio Beach, (4) San Lorenzo Beach, (5) Carranques Beach, (6) La Antilla Beach, (7) Castilla Beach, (8) La Barrosa Beach, (9) El Vendrell Beach. The symbol ⊕ gives the Puntal beach location in the northern coast. Position of the wave buoys: (a) Bilbao, (b) Gijón, (c) Sevilla, (d) Cádiz, (e) Tarragona.

2. Data set for model validation

The proposed model has been validated using field and experimental data obtained from four independent sources: (a) field and textural data from 11 beach profiles distributed along the Spanish coast (Fig. 1), ranging from micro- to macrotidal and exposed to different wave climate regimes, previously compiled by Gómez-Pina (1995) and Galofré (2001); (b) field and textural data of seasonally measured profiles on the Puntal Beach (northern coast of Spain); (c) wave climate data provided by the Spanish Grid of Measure and Record of Waves (REMRO) and the Ministry of Public Engineering and Transport (MOPT) and tidal data provided by the Spanish Grid of Tide Gauges (REDMAR); and (d) large wave channel data obtained in laboratory surveys performed by Peters et al. (1996) simulating tidal conditions.

2.1. Beach characteristics

The beaches were divided into three groups according to their topography and hydrodynamic environments. The first group comprises five beaches (Zumaia, Zarautz, Bakio, San Lorenzo

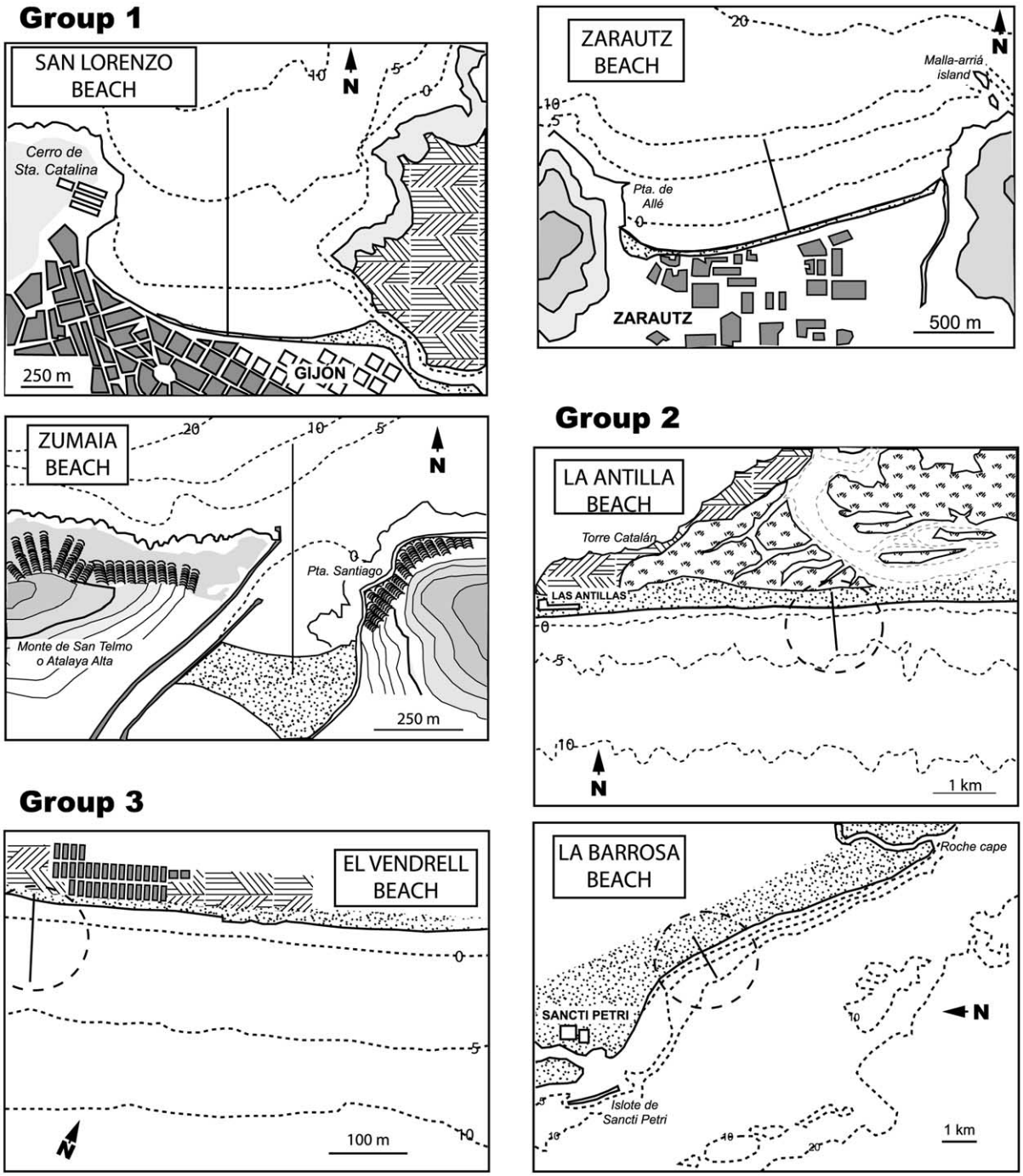

Fig. 2. Some examples of the configuration of the beaches studied

Table 1
Survey characteristics, wave climate (H_s = mean significant wave height of the month before the profile measurement, T = associated period), modal tidal range (TR) and grain size parameters corresponding to each beach studied

Beach	Beach length (m)	Measured profiles	Sediment samples	H_s (m)	T_p (s)	TR (m)	D_{50} (mm)		Ω_{sf}	Ω_{sh}
							Surf profile	Shoaling profile		
Group 1										
Zumaia	270	1	4	0.82	9.73	3.65	0.44	0.30	1.52	2.31
Zumaia (S)	270	1	4	2.56	12.67	3.65	0.44	0.30	3.64	5.55
Zarautz	2 500	10	8	1.94	12.68	3.65	0.35	0.25	3.55	5.14
Bakio	540	5	3	0.94	9.10	3.65	0.30	0.23	2.84	3.80
San Lorenzo	1 200	4	12	0.80	7.41	3.25	0.34	0.25	2.59	3.62
San Lorenzo (S)	1 200	4	12	2.3	11.68	3.25	0.34	0.25	4.71	6.61
Carranques	220	2	9	0.58	8.89	3.25	0.36	0.23	1.47	2.40
Group 2										
Castilla	24 000	42	9	0.63	6.95	2.65	0.35	0.20	2.10	3.89
La Antilla	16 000	4	9	0.76	9.71	2.65	0.35	0.22	1.81	3.02
La Barrosa	7 000	3	6	0.82	8.58	2.65	0.33	0.23	2.36	3.52
Group 3										
El Vendrell	12 000	21	6	0.54	6.9	0.40	0.27	0.19	2.41	3.55

The dimensionless fall velocity associated with the surf and shoaling profile is presented. (S) indicates storm conditions.

and Carranques) located on the Cantabrian coast of northern Spain. These beaches are embayed and their lengths vary between 200 and 2500 m (Fig. 2). For these beaches, the seasonal variability is mainly associated with cross-shore sediment transport. The number of measured profiles varies as a function of the length and characteristics of each beach (Table 1. A representative profile is selected from the central part of each beach, assuming that the wave evolution in this part of the beach is better controlled by the bathymetry and sediment characteristics than by topographic sheltering effects. The second group includes the Castilla, La Antilla and La Barrosa beaches on the Atlantic coast of southwest Spain (Fig. 2). This is a low coast with a general NNW–SSE alignment. These beaches are fairly linear with lengths of 24, 16 and 7 km, respectively. The third group is composed of a single beach, El Vendrell, located on the Mediterranean coast. This section of the coast is orientated NE–SW and is characterised by extensive linear beaches. In this beach the seasonal changes are associated with cross- and longshore sediment transport.

Sediment characterisation of studied beaches is quantified in terms of the median (D_{50}) of the grain size distribution. The number of samples collected depended on the length of the profile (Table 1). The grain size was estimated averaging the median values of the collected samples, defining a characteristic value for the intertidal and the subtidal zones (Table 1). The dimensionless fall velocity was defined for each section, named Ω_{sf} for the surf profile and Ω_{sh} for the shoaling profile. Comparing these parameters, a useful relationship was established that indirectly relates the grain sizes in these two zones (Fig. 3):

$$\Omega_{sh} = 0.53 + 1.3\Omega_{sf} \quad (2)$$

This expression allows simplification of the model, representing data exclusively in terms of the intertidal dimensionless fall velocity Ω_{sf}. This is an important advantage for the practical application of our model.

The data from El Puntal beach have been used to validate the predictive capacity of the model. This beach is located in the entrance to Santander Bay in the northern coast of Spain, forming part of a 3-km-long spit (Fig. 1).

2.2. Wave climate and tidal range

The wave climate was characterised using two different sources. Firstly, the wave parameters

provided by the REMRO buoys. In each beach, the closest scalar buoy was selected to define the wave conditions (Fig. 1). On the northern coast, the Bilbao and Gijón buoys were used for beaches in Group 1 and for El Puntal beach. For Group 2, the buoys of Cádiz and Sevilla were employed. The Vendrell beach wave data were extracted from the Tarragona buoy. The analysis of measured wave data provides a set of wave parameters (significant, mean, and maximum wave height and peak, zero-crossing and maximum period). For this study, the significant height (the most frequently used parameter in coastal studies) and peak spectral period (the most energetic period) were used. The values used correspond to the mean values of the month before the profile measurement (Table 1), which are the best values to fit the proposed equilibrium profile model.

Secondly, the most frequent direction of wave propagation was obtained from the code of Recommendations for Maritime Constructions (ROM), Appendix of Characterization of Wave Climate (0.3-91) on the Spanish coast (MOPT, 1992), where a wave climate characterisation of the Spanish coast is provided. The buoys are located in intermediate-depth water and, consequently, waves are propagated considering refraction, diffraction and shoaling processes from the most frequent direction. Finally, it should also be pointed out that the representative value is the wave height at the closure depth for each beach.

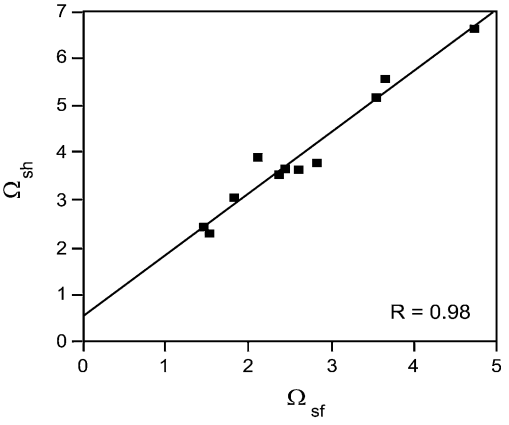

Fig. 3. Relationship between the dimensionless fall velocity associated with the intertidal and subtidal zones of the beach profile.

Table 1 presents the local wave height and peak period.

The beaches studied are in the range of micro- to macrotidal beaches (Davies, 1964), based on the spring tidal range. The modal tidal range considered was obtained from the Spanish Grid of tide gauges (REDMAR). The values corresponding to each beach are also presented in Table 1.

Considering these data sources, the general wave climate and tide conditions are described for the three groups of beaches. The Cantabrian coast and consequently the beaches of Group 1 are generally exposed to energetic swell waves from the north to northwest and are macrotidal beaches with modal tidal ranges up to 3 m. In contrast, Group 2, located at the south Atlantic coast of Spain, experiences sea and swell waves mainly from the west-northwest and west in deep water, the latter associated with storm winds in winter. The bathymetry and orientation of the coast modify wave fronts such that the approaching waves mainly reach the beaches with a SSW direction. The modal tidal range is around 2.65 m and these beaches are mesotidal. Finally, the north-Mediterranean coast where Group 3 occurs is characterised by sea, and less frequently, by swell waves coming from the northeast and southwest. The local topography in front of El Vendrell beach transforms the incident wave direction to arrive at the beach from the southeast. This coast is microtidal, subjected to a modal tidal range of 40 cm.

2.3. Laboratory studies

Field test validation of models assessing tidal influence on beach morphology is difficult to achieve, primarily because it is impossible to compare directly in nature the morphology of the same beach with and without tide. A few laboratory experiments (Watts and Dearduff, 1954; Saville, 1957; Kraus and Larson, 1988) have dealt with this problem incorporating a constant change of level as a well-constrained variable. For purposes here, the laboratory studies conducted by Peters et al. (1996) were considered. These experiments were performed in the Hannover wave channel which is 324 m long, 5 m wide

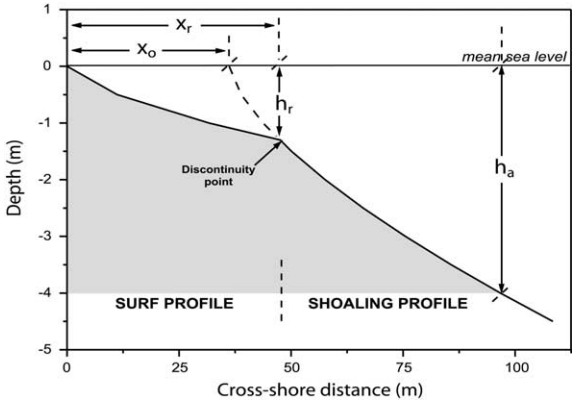

Fig. 4. The 2S-EBP. The figure illustrates the main parameters that define the model: x_r is the horizontal distance between the beginning of the surf profile and the discontinuity point; h_r is the discontinuity point depth in relation to the mean sea level; x_o is the horizontal distance between the beginning of the surf profile and the virtual origin of the shoaling profile over the mean sea level; and h_a determines the offshore limit of the model validity.

and 7 m deep, and able to generate waves of 2 m height. Irregular waves were simulated using a TMA spectrum. The median grain size was 0.33 mm for both the intertidal and subtidal zones. The most interesting aspect is that the surveys were developed for a constant level and for a changing water level. A sinusoidal tide of 1-m range with a 12-h period was simulated as a step function with increments of 25 cm every 60 min. High and low tide durations were 90 min. The survey began at high tide, which coincided with the mean sea level in the surveys without tide (4.5 m relative to the channel floor). The conditions for each case studied are presented in Table 2.

Table 2
Description of the survey parameters of the laboratory profiles measured by Peters et al. (1996)

Case	Wave parameters		Water level
	H_m (m)	T_p (s)	
1	1.20	5	Constant
2	1.20	10	Constant
3	1.10	5	Variable (1 m)
4	1.05	10	Variable (1 m)

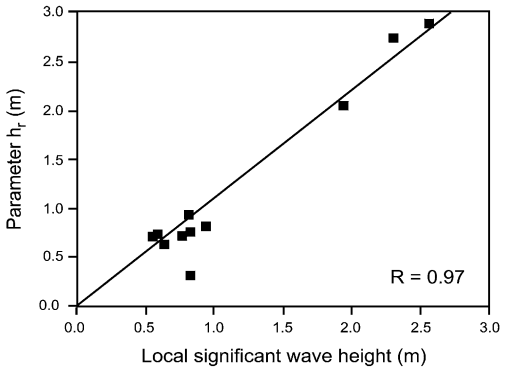

Fig. 5. Relationship between the depth of the discontinuity point, h_r, and the significant wave height that reaches the beach.

3. Theoretical basis: two-section equilibrium profile model

The 2S-EBP (Medina et al., 2000; Bernabeu et al., in press) is used as the basis of the morphological beach profile model presented here. The 2S-EBP assumes that the main wave energy dissipation process changes along the profile, from bottom friction to turbulence dissipation. Considering this and following the approach of Inman et al. (1993), a formulation for two separate sections, the surf and shoaling profiles, was developed (Fig. 4). Both sections join at the breaker point, to which we refer to from now on as the discontinuity point. This approach integrates the energy reflection from the beach in the equilibrium profile formulation, obtaining:

Surf profile :

$$x = \left(\frac{h}{A}\right)^{3/2} + \frac{B}{A^{3/2}}h^3 \quad 0 \le x \le x_r \tag{3}$$

Shoaling profile :

$$X = x - x_0 = \left(\frac{h}{C}\right)^{3/2} + \frac{D}{C^{3/2}}h^3 \quad x_r \le x \le x_a \tag{4}$$

The expressions above are similar for the surf and shoaling profiles and are composed as the sum of two terms. The first term coincides with the Dean (1977) profile expression. The second term appears when the reflection phenomenon is taken into account. It should be noted that the shoaling profile is displaced a distance x_o from the reference system situated on the shoreline.

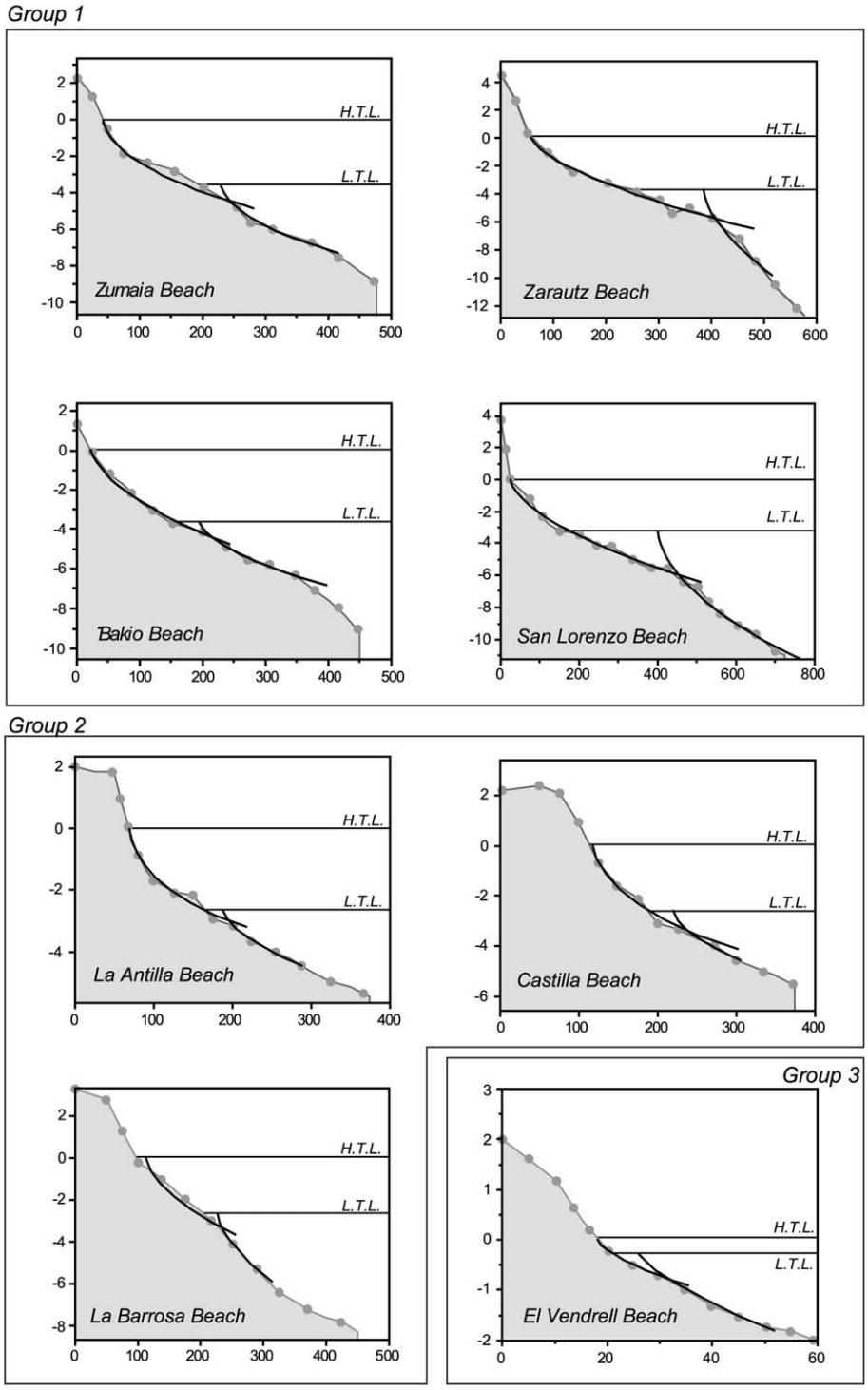

Fig. 6. Selected examples illustrating the goodness of fit to field-measured beach profiles. H.T.L. is the high tide level; L.T.L. is the low tide level.

Table 3
Fitting coefficients of the model to surf and shoaling profiles (A and C associated with energy dissipation and B and D related to reflection processes)

Beach	Shape coefficients				ε (%)	Morphological parameters		
	A ($m^{1/3}$)	B ($m^{-3/2}$)	C ($m^{1/3}$)	D ($m^{-3/2}$)		h_r (m)	$x_{o\ measured}$ (m)	$x_{o\ calculated}$ (m)
Group 1								
Zumaia	0.18	0.07	0.14	0.06	1.6	0.77	188	187.41
Zumaia (S)	0.155	0.02	0.23	0.02	2.0	2.88	321	316.06
Zarautz	0.12	0.005	0.25	0.008	0.7	2.06	326	326.41
Bakio	0.15	0.02	0.1	0.02	0.6	0.82	172	169.59
San Lorenzo	0.13	0.05	0.1	0.06	1.9	0.95	231	231.76
San Lorenzo (S)	0.13	0.015	0.2	0.02	0.7	2.75	375	327.04
Carranques	0.18	0.01	0.11	0.005	0.5	0.75	96	95.27
Group 2								
Castilla	0.15	0.03	0.17	0.01	0.8	0.64	114	113.77
La Antilla	0.19	0.09	0.12	0.09	0.7	0.73	103	101.15
La Barrosa	0.2	0.2	0.1	0.08	1.1	0.32	119	109.99
Group 3								
El Vendrell	0.14	0.05	0.2	0.01	0.05	0.72	7.75	17.10
Peters et al. (1996)								
Case 3	0.16	0.08	0.9	0.4	0.6	1.25	59	64.42
Case 4	0.17	0.16	0.5	0.1	1.9	0.95	49	52.91

The goodness of the fittings is estimated by:

$$\varepsilon(\%) = \frac{\sum (h_{mi} - h_{fi})^2}{\sum h_{mi}} \times 100$$

where h_m is the actual depth, and h_f is the depth predicted by Eq. 3 or 4. The morphological parameters h_r and x_o are obtained from the fittings. $x_{o\ calculated}$ is predicted by Eq. 13.

The 2S-EBP is defined by four shape coefficients. The first two are dimensional coefficients that depend on the energy dissipation, namely A ($m^{1/3}$) for the surf profile, and C ($m^{1/3}$), for shoaling profile, both appearing in the first term of Eqs. 3 and 4. The two other dimensional coefficients are functions of the reflection process; namely B ($m^{-3/2}$) in the surf profile and D ($m^{-3/2}$) in the shoaling profile, characterising the second term of the same set of equations. The last coefficients become zero ($B \approx 0$, $D \approx 0$) on dissipative beaches, with mild slopes and low energy reflection. In this case, the proposed model is reduced to a Dean (1977) expression in each section, although with different coefficient values.

Furthermore, the 2S-EBP proposes a set of analytical expressions to define some of the morphological parameters of the model (Fig. 4). The parameter x_o that defines the distance between the beginning of the surf profile and the start of the shoaling profile is described as:

$$x_o = \left(\frac{h_r}{A}\right)^{3/2} - \left(\frac{h_r}{C}\right)^{3/2} + \frac{B}{A^{3/2}}(h_r)^3 - \frac{D}{C^{3/2}}h_r^3 \quad (5)$$

The vertical distance of the discontinuity point in relation to the mean sea level, h_r, is defined with an empirical criterion based on field data. This point coincides with the breaker point and, considering the wave breaking criteria, $H = \gamma h$, the depth h_r is related to the wave height that reaches the beach. The data agree with this relationship, as shown in Fig. 5:

$$h_r = 1.1 H_s \quad (6)$$

Knowing the depth h_r and using the surf profile formulation, Eq. 3, the distance from the discontinuity point to the shoreline, x_r, is expressed as (see Fig. 4):

$$x_r = \left(\frac{h_r}{A}\right)^{3/2} + \frac{B}{A^{3/2}}(h_r)^3 \quad (7)$$

The parameter h_a that defines the limit of the validity of the model assuming shallow-water lin-

ear wave theory (Fig. 4) is described using the criterion for shallow water, $h/L < 0.05$. Considering the deep water wavelength, L_o, with an error less than 5% (Komar, 1998) and the relation between wave height and wave period along Spanish coast, established by MOPT (1992), $T \approx 6\sqrt{H_S}$, the limiting depth of the model validity is:

$$h_a \approx 3H_S \quad (8)$$

According to this expression, the shoaling profile validity spans to a depth that is three times the significant wave height that reaches the beach profile.

The 2S-EBP was compared with the measured beach profiles outlined above, demonstrating its ability to describe the profile morphology (Fig. 6). Best-fit coefficients, obtained by iteration, are listed in Table 3. The empirical relationships between the shape coefficients (A, B, C and D) and the wave and sediment characteristics of the beach were established using the intertidal dimensionless fall velocity: $\Omega_{sf} = H_s/wT$ (Fig. 7). In the range $1 \leq \Omega \leq 5$, the relationships obtained are:

$$A = (0.21 - 0.02\Omega_{sf}) \quad (9)$$

$$B = 0.89 \exp[-1.24\Omega_{sf}] \quad (10)$$

$$C = (0.06 + 0.04\Omega_{sf}) \quad (11)$$

$$D = 0.22 \exp[-0.83\Omega_{sf}] \quad (12)$$

The empirical expressions in the surf profile, Eqs. 9 and 10, define an increase of the coefficients A and B as Ω_{sf} decreases. For values $\Omega_{sf} > 3$, the parameter B is in the order of 10^{-2}, the reflection term in the surf profile formulation, Eq. 3, represents less than 10% of the dissipation term for depths $h \leq 5$ m. The reflection effect on the beach is negligible. This range of Ω_{sf} values corresponds to intermediate-dissipative beaches (Wright and Short, 1984; Wright et al., 1985). In the shoaling profile, the parameter C increases as the beach approximates to dissipative state. Similarly to the coefficient B, the parameter D increases as Ω_{sf} decreases. For values $\Omega_{sf} > 3$, the coefficient D is also in the order of 10^{-2}, and the reflection term of the shoaling profile,

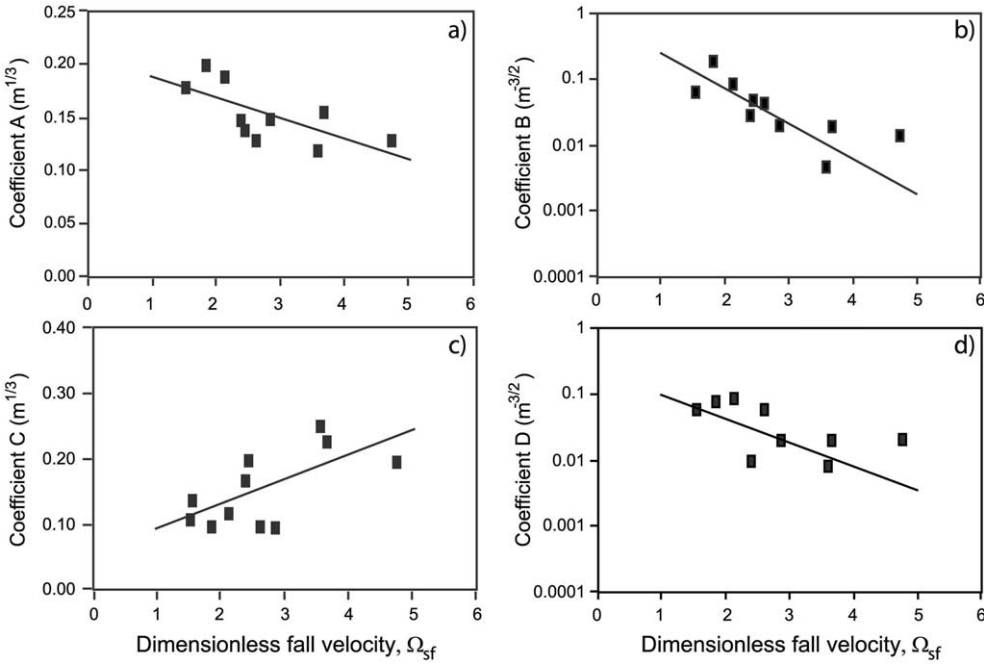

Fig. 7. The shape coefficients associated with the equilibrium profile as functions of the dimensionless fall velocity of the intertidal zone: (a) coefficient A; (b) coefficient B; (c) coefficient C; and (d) coefficient D.

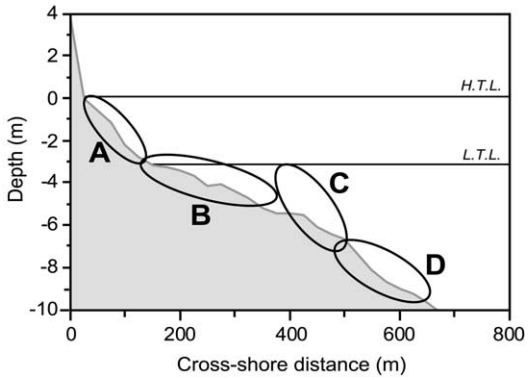

Fig. 8. Coefficients related to the slope in the upper and lower part of each section of the beach profile.

Eq. 4, represents less than 10% of the dissipation term for depths $h < 20$ m.

In the 2S-EBP, each section varies as a function of the relationship between the dissipation and reflection phenomena, with an upper and lower part (Fig. 8). This allows defining different degrees of concavity (Fig. 9). The dissipation coefficients (A in the surf profile and C in the shoaling profile) represent the slope in the shallower zone of each section. In this part, the coefficients increase with the slope. The reflection coefficients (B and D) define the slope in the deeper part. In this case, the coefficients increase as this part of each section flattens. Consequently, the empirical Eqs. 9–12 that relate the coefficients of the equilibrium profile, hydrodynamics and morphology describe the response of the surf and shoaling profiles under different wave and sedimentary conditions (Table 4).

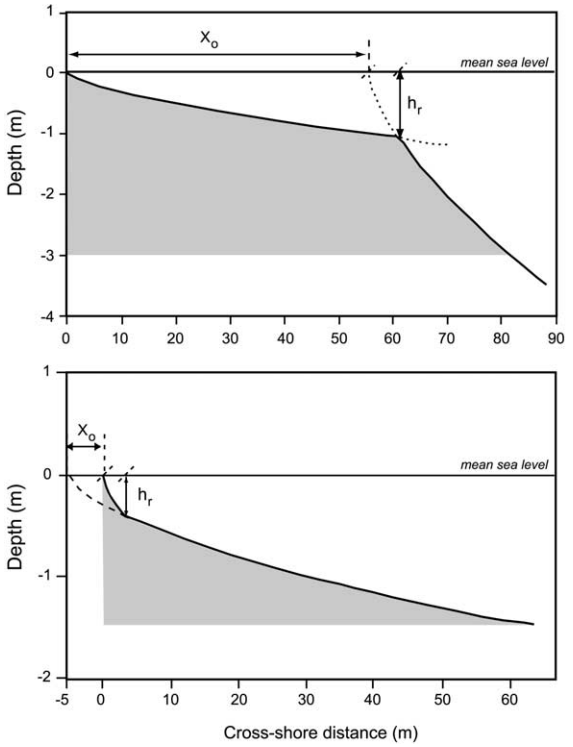

Fig. 9. Examples of the morphology prediction: (top) dissipative equilibrium profile; and (bottom) reflective equilibrium profile.

4. Tidal influence on beach morphodynamics

The 2S-EBP was proposed assuming a constant sea level. Based on this model, the effect of tide on beach morphology was analysed considering the relative importance of wave processes (swash, wave breaking and shoaling) that affect the beach

Table 4
Descriptive relationships between the dimensionless fall velocity (including hydrodynamic and sedimentary conditions), the proposed equilibrium profile (coefficient behaviour) and the resultant morphology

Condition	Section	Shape coefficient	Morphological feature
Dissipative, $\uparrow \frac{H}{wT}$	Surf profile	$\downarrow A$	Flattened upper part
		$\downarrow\downarrow B$	Steep lower part
	Shoaling profile	$\uparrow C$	Steep upper part
		$\downarrow\downarrow D$	Steep lower part
Reflective, $\downarrow \frac{H}{wT}$	Surf profile	$\uparrow A$	Steep upper part
		$\uparrow B$	Flattened lower part
	Shoaling profile	$\downarrow C$	Flattened upper part
		$\uparrow D$	Flattened lower part

profile. Bernabeu et al. (2002b) demonstrated that the 2S-EBP for tidal beaches coincides with the formulation for beaches considering a constant sea level (Eqs. 3 and 4). Fig. 10 shows the 2S-EBP for tidal beaches. This model was tested against field data measured along the Spanish coast (Fig. 6) and laboratory tidal profiles measured by Peters et al. (1996) (Fig. 11).

Consequently, the 2S-EBP describes the same morphology of the surf and shoaling profile for tidal and non-tidal beaches. The values of the four coefficients A, B, C and D remain constant, and their influence on the profile morphology is preserved. However, some differences appear in the application of the model in each case, including the limits of the surf profile change. In tideless beaches the surf profile extends between the mean sea level and the breaker point. In tidal beaches, it spans from the high tide level to the breaker point at low tide level. The larger the tidal range, the longer the surf profile (Fig. 10). In tidal beaches, the discontinuity point corresponds to the breaker point at low tide. Obviously, this involves a change in the expression of the parameter x_o. In the tidal case, x_o is the horizontal distance between the beginning of the surf profile and the virtual origin of the shoaling profile over a new reference: the low tide level (Fig. 10). This is reflected in the expression of x_o where the tidal range, TR, is included:

$$x_o = \left(\frac{h_r + TR}{A}\right)^{3/2} - \left(\frac{h_r}{C}\right)^{3/2} + \frac{B}{A^{3/2}}(h_r + TR)^3 - \frac{D}{C^{3/2}}h_r^3 \quad (13)$$

As the reference system is located on the high tide level, the depth of the discontinuity point is defined as h_r plus the tidal range. Knowing the wave height and the tidal range in a beach, the 2S-EBP provides a criterion for locating the position of the beginning of the shoaling profile. Fig. 12 shows the calculated and measured values of parameter x_o, demonstrating the goodness of fit of Eq. 13 to predict this parameter in tidal

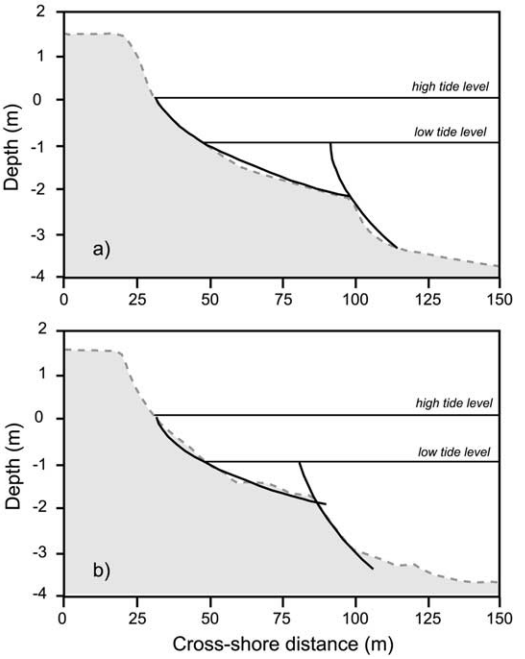

Fig. 11. Equilibrium profile fitting of the tidal laboratory profiles provided by Peters et al. (1996): (a) Case 3; (b) Case 4.

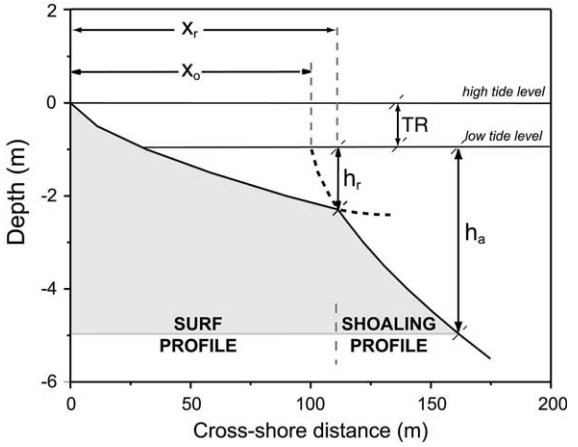

Fig. 10. General 2S-EBP, including the tidal range. The main morphological parameters for tidal beaches: x_r is the horizontal distance between the beginning of the surf profile and the discontinuity point; h_r is the discontinuity point depth in relation to the low tide level; x_o is the horizontal distance between the beginning of the surf profile and the virtual origin of the shoaling profile over the low tide level; h_a determines the depth in relation to the low tide level of the offshore limit of the model validity; and TR is the modal tidal range.

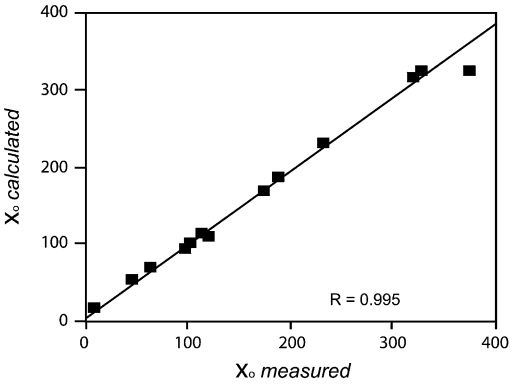

Fig. 12. Comparison of the analytical expression of the parameter x_o (Eq. 13) and the measured values of this parameter.

beaches. The linear fit between them is given by the expression:

$$x_{o\ calculated} = 0.96 x_{o\ measured} \quad (14)$$

Another difference derived from the above is the position of the discontinuity point, which separates the surf and shoaling profiles (Fig. 10). In tidal beaches, this discontinuity always remains submerged at a depth h_r below the low tide level, which is a function of the significant wave height at the closure depth of the beach (Eq. 6). Fig. 5 shows the relationship between these two parameters. The linear fitting justifies that the vertical position of the discontinuity point is mainly controlled by waves, and that the tidal influence results in the horizontal displacement associated with the surf profile stretching.

For tidal beaches, the wave breaking controls all the surf profile and the wave shoaling controls the profile offshore the breaker point during low tide. Consequently, the main tidal influence on the beach morphodynamics is the lengthening of the surf profile proportionally to the tidal range, maintaining the discontinuity point always submerged (Fig. 13). Beaches under the same wave and sedimentary conditions, but under different tidal range, show the same equilibrium profile but different surf profile length. The 2S-EBP is valid for micro-, meso- and macrotidal beaches. The parameter x_o is the unique element in the equilibrium beach profile that changes to incorporate the tidal range.

5. The predictive capacity of the 2S-EBP model

The proposed equilibrium profile model together with the empirical expressions obtained for coefficients A, B, C and D, allows definition of the equilibrium morphology of the profile. Its correct formulation is obtained after the value of the coefficients is estimated from the dimensionless fall velocity, Ω. Consequently with this, the reliability of the model to formulate the different equilibrium profiles that a given beach may attain after its exposure to seasonally distinct wave–climate conditions can be explored.

It is in this sense that the potentially predictive capabilities of the model have been evaluated against an independent data set obtained from El Puntal beach (northern Spain). The data set comprises the profile measurements at different times in the year, providing a record of its season-

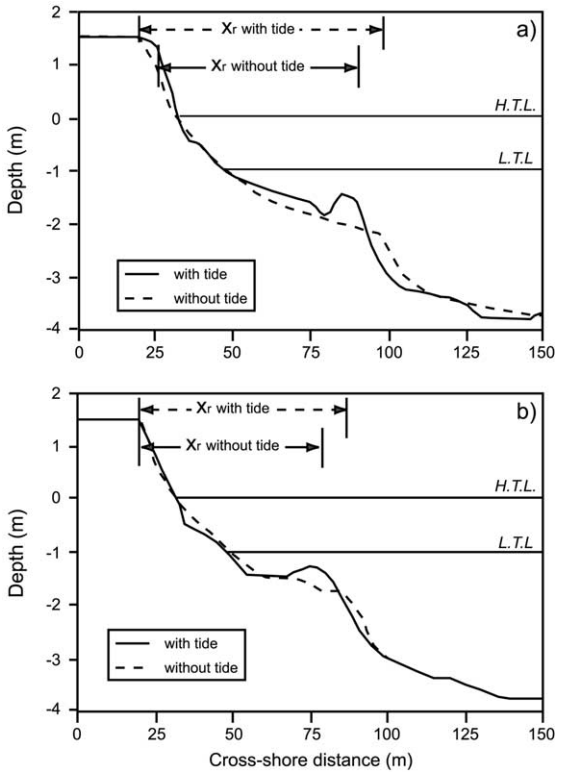

Fig. 13. Description of the tidal effect on the beach morphology through comparison of Peters et al. (1996) profiles with and without tide: (a) Cases 1 and 3; (b) Cases 2 and 4.

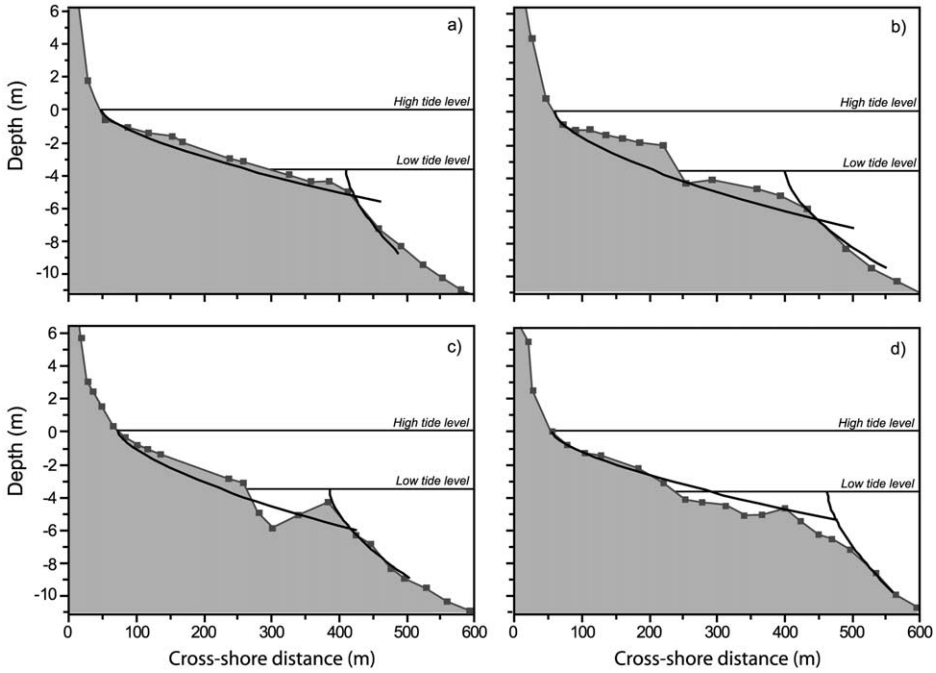

Fig. 14. Comparison between the predicted equilibrium profile calculated from Eqs. 3 and 4 against measured profiles in El Puntal beach at different times of the year. The empirical Eqs. 9–12 were used to estimate the model coefficients. The beach profiles were measured in (a) May 1990; (b) July 1990; (c) December 1990; and (d) January 1991.

al variability. Table 5 presents the values for grain size, wave height and wave period for the duration of the beach monitoring period. The values for coefficients A, B, C and D (Table 5) were calculated from Eqs. 9–12 and used to formulate their corresponding equilibrium profile, accordingly with the Eqs. 3 and 4.

Fig. 14 presents the predicted profile plotted against the measured profile in El Puntal beach in May, July, December of 1990 and in January of 1991. In general terms, both the calculated surf and shoaling profiles are in acceptable agreement with the actual profile, with errors around 10%. It should be noted that the selection of the significant wave height used to estimate the dimensionless fall velocity becomes of fundamental importance when exploiting the predictive capabilities of the model. In fact the significant wave height value is critical to obtain the best possible prediction of the surf profile, the most active part of the profile throughout the year. Nevertheless, the El Puntal beach data set provides a useful, if limited,

Table 5
Data corresponding to the profile measured in El Puntal beach

	Grain size, D_{50}	Fall velocity, w	H_s	T_p	Ω_{sf}	ε	Model coefficients			
	(mm)	(m/s)	(m)	(s)		(%)	A ($m^{1/3}$)	B ($m^{-3/2}$)	C ($m^{1/3}$)	D ($m^{-3/2}$)
May 1990	0.265	0.03175	1.92	9.58	5.50	5.0	0.10	0.0009	0.28	0.0023
July 1990	0.258	0.03083	1.31	9.21	3.98	21.6	0.13	0.0064	0.22	0.0081
December 1990	0.294	0.03559	1.68	9.86	4.19	9.9	0.13	0.0049	0.23	0.0068
January 1991	0.215	0.02997	2.13	11.02	5.80	9.2	0.09	0.0007	0.29	0.0018

H_s correspond to mean significant wave height of the month before the profile measurement propagated to the closure depth of the beach. The coefficients of the model were obtained using Eqs. 9–12.

insight into the predictive capabilities of the proposed model.

6. Discussion: an integrated morphological model of beach profile

Most equilibrium beach profile formulations relate the profile morphology exclusively to the grain size (Moore, 1982; Dean, 1987; Muñoz-Pérez et al., 1999; Bernabeu et al., 2002a). The 2S-EBP established that the profile morphology is also controlled by waves and tide in addition to the sediment characteristics, obtaining a number of empirical relations between the equilibrium profile and dynamic parameters (Table 4). The 2S-EBP has the ability to predict the beach profile under different wave and sedimentary conditions, making it a useful tool for coastal management applications. Once the variables that control the equilibrium profile for a given instant have been established, we need to establish how these parameters change over time, and how these changes have a significant influence on the profile morphology through time.

On a beach, the grain size varies along the profile. However, most equilibrium profile models can be related to the median of the grain size distribution, considering that as a representative value of the beach grain size. Losada et al. (1992) found seasonal grain size changes related to differential transport along the profile. Each grain size fraction is redistributed in a different way, modifying the grain size distribution of each part. Medina et al. (1995) defined the 'master sample' as the sum of all samples collected along a single profile. They observed that its grain size was constant over time. Consequently, and for the seasonal time scale, it is reasonable to assume the grain size as a constant.

However, the dynamic parameters, waves and tide, change sharply and distinctly with time. Tide, in particular, has a different temporal-scale variability. Considering the semidiurnal inequality, tide is a rapidly varying (in the order of hours) and not very energetic phenomenon. Consequently the profile morphology is not able to respond instantaneously to this type of sea level change and would need days or weeks to adapt to each new situation. For a larger temporal scale, Wright et al. (1982) and Masselink and Short (1993) have studied the monthly variation associated with the lunar cycle, and concluded that the impact of spring to neap tide is secondary relative to more energetic processes such as waves, and that the tidal variation does not significantly modify the beach morphology. In this sense, our morphological model tends to consider the tidal range more as a local variable (changing from one beach to another) than a temporal one (in a given beach over time).

It has previously been discussed to some degree that the variations in wave conditions are the principal cause of the main morphodynamical changes in the beach profile. In this sense, Short (1987) established that wave height is the major variable involved in temporal beach changes, considering that wave period is constant. Even as tide range increases, waves remain the main processes that control temporal beach change; however, the rate of beach change diminishes (Masselink and Short, 1993). Taking this into account, our morphological model is developed under the assumption that the beach profile is able to reach an equilibrium state under each dominant wave and tide condition, i.e. that the profile has enough time to develop completely in each situation.

Keeping these considerations in mind, the 2S-EBP allows prediction of morphological changes of the beach profile in response to variations in wave climate, as a function of the dimensionless fall velocity parameter: $\Omega = H/wT$, and for beaches subject to different tidal ranges. Based on this, we propose a morphological model of the beach profile (Fig. 15). We have followed the concept of Masselink and Short (1993), and used two axes to express the variations undergone by the main parameters (tide and waves).

The vertical axis describes the modal tidal range, TR, in a beach distinguishing between microtidal (<2 m), mesotidal (2–4 m) and macrotidal (>4 m), following Davies' (1964) classification. Since the tidal effect on the beach profile is restricted to a lengthening of the surf profile proportional to the tidal range, this differentiation responds more to the classification of the possible

environments than to the existence of important morphological differences between tidal situations.

On the horizontal axis, the dimensionless fall velocity mainly describes the variations of wave climate. In this case the threshold values given by Masselink and Short's (1993) model are used. Consequently, since the modal tidal range is assumed to be a constant parameter for a given beach, the dimensionless fall velocity should be sufficient to describe the seasonal variations of the beach profile.

6.1. Behaviour of the shape coefficients

During its seasonal variation, the beach profile evolves from an erosive state associated with energetic conditions and large values of Ω, to shoreline advancement conditions related to fair weather and small values of Ω. This transition is similar for the different tidal states. The study of the morphological changes is based on the empirical relationships obtained for the 2S-EBP (Table 4).

In the dissipative state ($\Omega > 5$), the reflection coefficients of the equilibrium profile (B and D) approach zero, and the morphology is controlled by energy dissipation. In this particular case, the equilibrium profile expressions for the surf and shoaling sections are reduced to the Dean (1977) expression. The coefficient A takes a low value whilst the coefficient C is at its maximum value (Fig. 7). A flattened surf section and a steepened shoaling section (Fig. 15, dissipative situation) then characterise the morphology of the profile. In this case, the discontinuity point is clear and easy to identify.

As Ω decreases associated with mild wave conditions, the shape coefficients reflect a significant change in the profile morphology (Fig. 7) also smoothing the discontinuity point. The reflection coefficients increase describing flattened lower parts for each section. The coefficient A increases as Ω decreases, giving a steepened slope in the upper part of the surf profile. The surf profile increases in curvature as it moves toward accumulative situations (Fig. 15, along horizontal axis). At the same time, the coefficient C decreases with Ω. This results in the flattening of the upper and lower parts of the shoaling profile. The break in the slope associated with the discontinuity point becomes gradually smoother. Microtidal beaches represent an extreme case in which the surf profile in the intermediate and reflective state is reduced to the beach face, and their lower part disappears (Fig. 15). In this way, the shoaling profile appears an extension of the surf profile, seeming a unique curve.

The 2S-EBP and associated empirical relationships describe the equilibrium profile associated with each morphodynamic state defined by Ω and predict the morphological beach changes. Even more, using the complete expressions of 2S-EBP (Eqs. 3 and 4), it is possible to define different degrees of concavity in each section, improving the approximation from the dissipative to the reflective profile shape. This allows integration of this equilibrium profile in the widely used morphodynamics model of Wright and Short (1984) for microtidal beaches.

6.2. Behaviour of the morphological parameters

Fig. 10 shows the 2S-EBP for tidal beaches with the main morphological parameters that describe the beach profile. The parameter h_r is the depth of the discontinuity point relative to the low tide level. In Fig. 5, the wave height and the depth of the discontinuity point are plotted, establishing the linear relationship between them (Eq. 6). Considering this fitting equation, under winter conditions (large values of Ω), the discontinuity point is located fairly deep below the low tide level. If we move along the horizontal axis of the model, in the direction of decreasing Ω, Eq. 6 defines a shallower discontinuity point with decreasing wave height. Consequently, the variation of the dimensionless fall velocity, Ω, generates a vertical displacement of the discontinuity point. In Fig. 15, the parameter h_r remains constant along a tidal axis. For a given Ω value, the depth of the discontinuity point relative to the low tide level remains independent of the tidal range.

Considering that the model is based on shallow-water linear wave theory, the validity of the model is limited by the vertical distance h_a as shown in Fig. 10 and as the shaded zone in Fig.

15. This parameter is approximately three times the significant wave height (Eq. 8). A decrease in Ω associated with a wave height decrease modifies the position of the validity limit of the 2S-EBP. In the dissipative state, h_a reaches the maximum value, decreasing with wave height toward more intermediate and reflective situations.

The parameter x_o is the distance between the beginning of the surf and the shoaling profile (Fig. 10). This parameter presents different behaviour for micro-, meso- and macrotidal beaches. In microtidal beaches, TR < 2 m, the parameter x_o reaches maximum values in the dissipative state, when the profile slope is flattest and the surf profile progressively becomes shorter as it evolves toward reflective conditions. There is an extreme situation in reflective tideless beaches, as the parameter x_o become negative, implying that the beginning of the shoaling profile is situated behind the coastline (Fig. 9, bottom).

The behaviour of the parameter x_o changes as the tidal range increases. For meso- and macrotidal beaches, the dissipative state results in large values of x_o. In Eq. 13, the term associated with the energy dissipation in the surf profile, $[(h_r+TR)/A]^{3/2}$, is more dominant in this state, since the coefficient A reaches the minimum values (Fig. 7a). The terms related to the shoaling profile are small because of the maximum values of the coefficient C for dissipative beaches. In the intermediate state ($2 < \Omega < 5$), x_o decreases following the same tendency as for microtidal beaches. In contrast, in the reflective state ($\Omega < 1$), the tendency of the parameter x_o changes, increasing as Ω decreases. In this case the term associated with energy reflection in the surf profile, $(B/A^{3/2})(h_r+TR)^3$, determines the value of x_o, since this state defines the maximum value of B and minimum of A. The reflective profile has a steepened initial part but offshore, the lower part is extremely flat. Consequently a small increment in tidal range causes a substantial increase in the surf profile length. In the extreme case of macrotidal beaches, the parameter x_o becomes higher for reflective than for dissipative beaches. In this situation, macrotidal reflective beaches, our equilibrium beach profile is capable of describing the beach morphodynamics variation with tide described by Wright et al. (1982). Whilst the steepened upper part of the surf profile generates reflective conditions and a narrow surf zone in high tide, during low tide the flattened and lengthened lower part of the surf profile results in dissipative conditions and a wide surf zone.

The parameter x_r is the distance between the beginning of the surf profile and the discontinuity point (Fig. 10). The behaviour of this parameter is similar to the parameter x_o. The parameter x_r decreases with Ω on microtidal beaches. In meso- and macrotidal beaches the parameter x_r diminishes from the dissipative to the intermediate state, and increases from there to the reflective state.

6.3. Implications of the proposed model

Our beach evolution model is based on the concept of equilibrium beach profiles, whilst preceding morphodynamics models (Wright and Short, 1984; Masselink and Short, 1993) use empirical data and describe a 3D morphodynamics states. We are able to represent the first-order morphological characteristics, that is, the mean slope and the concavity in each section. Consequently, second-order morphological features such as bars, ridges and cusps are not expressed in our model. Although on microtidal beaches the presence of nearshore bars is frequent and incorporated in several of the morphodynamics states described by Wright and Short (1984), the tidal sweep effect on the beach profile inhibits bar generation in the surf zone (Watts and Dearduff, 1954; Hedegaard et al., 1991). If an important effect of tides is the smoothing of the beach profile, then the 2S-EBP can be regarded as an appropriate method of describing and predicting the tidal beach profile under different wave conditions.

Fig. 15 shows the morphological model, describing the equilibrium profile for each condition. The shaded zone defined by h_a represents the validity of the assumptions of shallow-water linear wave theory. Bernabeu (1999) demonstrated that the depth h_a was situated in the shoaling zone described by Hallermeier (1981) where the annual changes of the beach profile are very

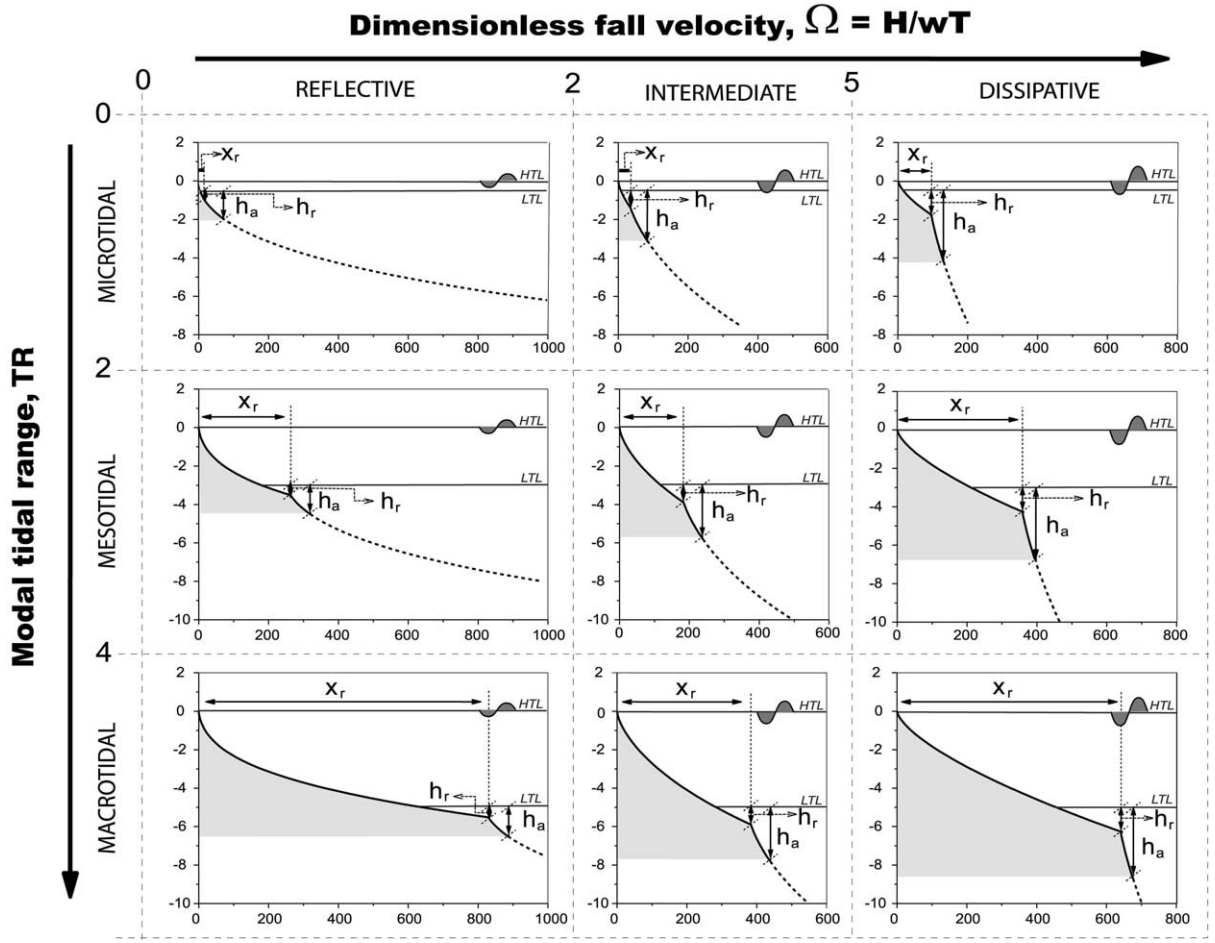

Fig. 15. Morphological beach profile model. The profile morphology depends on the dimensionless fall velocity, Ω, and the modal tidal range, TR. The shaded area represents the zone of validity of the 2S-EBP. Offshore this point, the initial hypothesis of the model is invalid.

small. This parameter h_a decreases from the dissipative to the intermediate and reflective situations. In this transition, waves mainly rework the part of the profile above the depth h_a in each condition. In deeper waters, waves have less influence on the profile morphology, and the deeper part of the profile associated with more energetic conditions remains unmodified in the reflective stage (summer profile). In the general model (Fig. 15), the *relict* profile associated with the more energetic conditions is not reflected. For illustration purposes, Fig. 16 presents a numerical example of the final profile morphology after a transition from dissipative ($\Omega = 6$) to intermediate

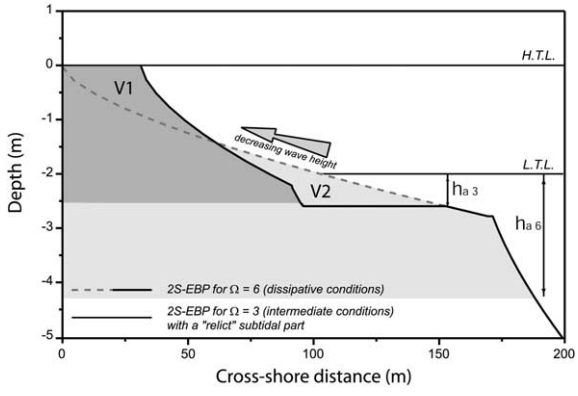

Fig. 16. Numerical example of the morphological transition from dissipative ($\Omega = 6$) to intermediate ($\Omega = 3$) conditions.

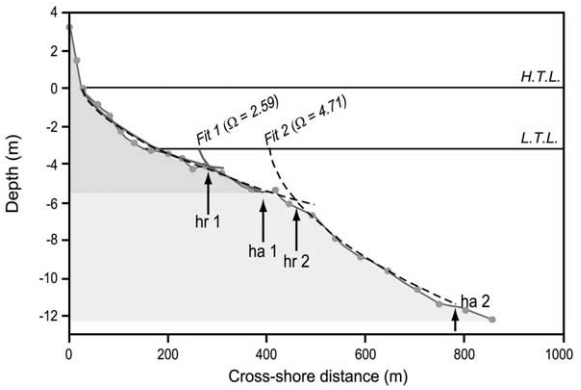

Fig. 17. San Lorenzo beach profile for which it is possible to distinguished a *relict* profile related to more energetic conditions. In this case, two fittings are necessary for each wave condition.

conditions ($\Omega = 3$), assuming that the total sand volume remains constant ($V_1 = V_2$). The differences in the parameter h_a associated with the changes in wave height appear as a set of slope discontinuities. An example of this is shown by the San Lorenzo beach profile (Fig. 17), where the discontinuities associated with the different wave conditions are well marked, requiring two equilibrium beach profiles to be fitted.

The 2S-EBP used in the morphological beach profile model includes the tidal effect on beach morphology, concluding that the surf profile in tidal beaches spans from the high tide level to the breakpoint during low tide. The model considers that wave breaking completely controls the intertidal zone. This assumes that the relative importance of each process is not determined by the time interval that each acts on the profile, but by the relative energy level of each independent process (Masselink and Short, 1993).

Increasing the tidal range, the most energetic swash and surf zone processes become less important as Masselink (1993) has confirmed. The field data obtained by Wright et al. (1982), Jago and Hardisty (1984) and Horn (1993) in beaches with tidal ranges of 9.5, 7.5 and 5.5 m respectively, show that the morphology in the low tide zone of the profile (the deeper part of our surf profile) is controlled by the shoaling waves. However, Wright et al. (1982) calculated the dissipation rates over half a lunar tidal cycle. For small waves with $H_o = 0.5$ m and a tidal range of TR = 9.5 m, the energy dissipation by surf zone waves in the low tide zone was not less than 20% of the total. This raises the question of the limit where the morphology is dominantly controlled by surf or by shoaling. The relative importance of the different processes on beach morphodynamics should be given by the relationship between the energy level and the time interval that each process acts on a given point of the beach profile. Somehow, the relation between tidal range and wave height, RTR, proposed by Masselink and Short (1993) could be used to define the predominant processes in each part of the profile. In this way, RTR can be redefined as a useful parameter to describe the hydrodynamic conditions more than to define the morphology of a beach profile. We will illustrate this considering two different situations, a reflective microtidal beach (TR = 1 m and $H = 1$ m) and a dissipative macrotidal beach (TR = 4 m and $H = 4$ m). Both of them have the same value of RTR = 1, and we could assume that the surf zone waves mainly control the complete morphology of the surf profile, but the equilibrium profile morphology in each case is very different, as shown in Fig. 15. The establishment of threshold values is still necessary to discriminate the different influences of the swash, surf zone and shoaling processes. If this objective could be achieved, the application of our beach evolution model in particular and the understanding of tidal beach behaviour in general would be improved.

7. Conclusions

This study models the general behaviour of tidal beaches subjected to different wave conditions. It presents a morphological model based on the equilibrium beach profile that relates the beach profile morphology with hydrodynamic and sedimentological parameters.

The dimensionless fall velocity and the modal tidal range are the main parameters of the model. Tide is considered to be a spatial variable. That is, its effect is important between different beaches, but negligible for a particular beach over time, because, in fact, the beach response time is longer

than the tidal period. Consequently, wave climate, and more specifically wave height, is the principal temporal variable controlling the seasonal beach morphology.

The 2S-EBP and associated empirical relationships provide the basis of a model capable of describing the morphology of the beach profile and potentially of predicting its seasonal change. For different dimensionless fall velocities, the 2S-EBP provides distinctive profile morphologies. From dissipative to reflective conditions, a flattened surf profile and a steepened shoaling profile transform to a concave surf profile and a flattened shoaling profile. When tide is introduced, the applicability and scope of this model broaden. The daily sea level change generates a lengthening of the surf profile, maintaining the equilibrium profile shape constant.

It has been demonstrated that the proposed model has some predictive potential. Knowing the dimensionless fall velocity and the modal tidal range, it is possible to calculate the four coefficient values, and substituting them in the 2S-EBP formulations, to define the profile shape related to a given set of conditions. This capability has been validated with limited data, giving a good qualitative approximation. However, further development of its full predictive capabilities should be based on a broader data set to produce a robust and quantitatively well-constrained validation.

The morphological model based on the equilibrium situation provides a feasible framework to understand the first-order behaviour of beaches under the action of waves and tides. Its simplicity should provide a good state-of-the-art tool for coastal management and prediction of equilibrium beach profiles under diverse wave and tide conditions. However, we must stress that considerable additional improvement is required, not only in the application of this model, but in the general understanding of tidal beaches. To fully achieve this goal it will be necessary to establish with rigor the relative importance of the hydrodynamic processes (swash, surf zone and shoaling processes) that control profile morphology. The relation between tidal range and wave height, RTR, seems a good parameter to describe this important threshold, but the dimensionless fall velocity plays a most important role in the discrimination of different type states, even in tidal beaches.

Acknowledgements

The measured data have been kindly provided by the Dirección General de Costas (Spain). Thanks to D. Rey for providing useful ideas and revising the English version of the manuscript. Also many thanks to Prof. R.G. Dean and an anonymous reviewer for their constructive comments that greatly improve the original manuscript. Contribution number 271 to the projects: REN2000-1102MAR (CICYT), PGIDT00PXI-30105PR and PGIDT00MAR30103PR (Xunta de Galicia) and IGCP 464. R.M. and C.V. acknowledge the financial support received from European Community through Project MAS3-CT97-0081, 'Surf and Swash Zone Mechanics' (SASME) and from the CICYT, Project AMB99-0543.

References

Bagnold, R.A., 1940. Beach formation by waves: some model experiments in a wave tank. J. Inst. Civil Eng. 15, 27–52.

Bascom, W.N., 1951. The relationship between sand size and beach face slope. Trans. AGU 32, 866–874.

Benavente, J., Gracia, F.J., López-Aguayo, F., 2000. Empirical model of morphodynamics beachface behaviour for low-energy mesotidal environments. Mar. Geol. 167, 375–390.

Bernabeu, A.M., 1999. Desarrollo, validación y aplicaciones de un modelo general de perfil de equilibrio en playas. PhD Thesis, Universidad de Cantabria, Santander.

Bernabeu, A.M., Muñoz-Pérez, J.J., Medina, R., 2002a. Influence of rocky platform in the beach profile morphology: Victoria Beach, Cádiz. Ci. Mar. 28, 181–192.

Bernabeu, A.M., Medina, R., Vidal, C., 2002b. An equilibrium profile model for tidal environments. Sci. Mar. 66, 325–335.

Bernabeu, A.M., Medina, R., Vidal, C., in press. Wave reflection on natural beaches: an equilibrium profile model. Estuar. Coast. Shelf Sci. 56, in press.

Bodge, K., 1992. Representing equilibrium beach profiles with an exponential expression. J. Coast. Res. 8, 47–55.

Bowen, A.J., 1980. Simple models of nearshore sedimentation: Beach profiles and longshore bars. In: McCann, S.B. (Ed.), The Coastline of Canada. Geological Survey of Canada, 80-10, pp. 1–11.

Brunn, P., 1954. Coast erosion and the development of beach profiles. Beach Erosion Board Tech. Mem. 44.
Carter, R.W.G., 1988. Coastal Environments. Academic Press, London, 617 pp.
Clarke, D.J., Eliot, I.G., Frew, J.R., 1984. Variation in subaerial beach sediment volume on a small sandy beach over a monthly lunar tidal cycle. Mar. Geol. 58, 319–344.
Dalrymple, R.A., Thompson, W.W., 1977. Study of equilibrium beach profile. Proceedings of the 15th International Conference on Coastal Engineering, ASCE, pp. 1277–1296.
Davies, J.L., 1964. A morphogenic approach to world shorelines. Z. Geomorphol. 8 (Mortensen Sonderheft), 127–142.
Davis, R.A., Hayes, M.O., 1984. What is a wave-dominated coast? Mar. Geol. 60, 313–329.
Dean, R.G., 1973. Heuristic models of sand transport in the surf zone. Proceedings of the First Australian Conference on Coastal Engineering, Engineering Dynamics on the Surf Zone, pp. 208–214.
Dean, R.G., 1977. Equilibrium beach profiles: U.S. Atlantic and Gulf coasts. Ocean Eng. Tech. Rep. 12, University of Delaware, Newark, DE.
Dean, R.G., 1987. Coastal sediment processes: toward engineering solutions. Proceedings of the Specialty Conference on Coastal Sediments '87, ASCE.
Dean, R.G., 1991. Equilibrium beach profiles: Characteristics and applications. J. Coast. Res. 7, 53–84.
Duncan, J.R., 1964. The effects of watertable and tide cycle on swash-backwash sediment distribution and beach profile development. Mar. Geol. 2, 186–197.
Eliot, I.G., Clarke, D.J., 1988. Semidiurnal variation in beachface aggradation and degradation. Mar. Geol. 79, 1–22.
Everts, C.H., 1978. Geometry of profiles across inner continental shelves of the Atlantic and Gulf coasts of the United States. Tech. Pap. 78-4, Coastal Engineering Research Center, US Army Corps of Engineering, Fort Belvoir, VA.
Fenneman, N.M., 1902. Development of the profile of equilibrium of the subaqueous shore terrace. J. Geol. X, 1–32.
Foote, Y., Russell, P., Huntley, D., Sims, P., 1998. Energetics prediction of frequency-dependent suspended sand transport rates on a macrotidal beach. Earth Surf. Proc. Landforms 23, 927–941.
Galofré, J., 2001. Desarrollo y validación de un modelo de distribución granulométrica de sedimentos en playas. PhD Thesis, Universidad de Cantabria, Santander.
Gómez-Pina, G., 1995. Análisis de los perfiles de playa en la fachada cantábrica y atlántica de la costa española y su aplicación a proyectos de regeneración. MSc Thesis, Universidad de Cantabria, Santander.
Hallermeier, R.J., 1981. A profile zonation for seasonal sand beaches from wave climate. Coast. Eng. 4, 253–277.
Hedegaard, I.B., Deigaard, R., Fredsoe, J., 1991. Onshore/offshore sediment transport and morphological modelling of coastal profiles. Proceedings of Coastal Sediments '91, pp. 643–654.
Horn, D.P., 1993. Sediment dynamics on a macrotidal beach: Isle of Man, U.K. J. Coast. Res. 9, 189–208.
Inman, D.L., Elwany, M.H., Jenkins, S.A., 1993. Shorerise and bar-berm profiles on ocean beaches. J. Geophys. Res. 98 (c10), 18181–18199.
Jago, C.F., Hardisty, J., 1984. Sedimentology and morphodynamics of a macrotidal beach, Pendine Sands, SW Wales. Mar. Geol. 60, 123–154.
Johnson, J.W., 1956. Dynamics of nearshore sediment transport. Bull. Am. Assoc. Pet. Geol. 40, 2211–2232.
King, C.A.M., 1972. Beaches and Coasts. Edward Arnold, London.
Komar, P.D., 1998. Beach Processes and Sedimentation. Prentice Hall, Englewood Cliffs, NJ.
Komar, P.D., McDougal, W.G., 1994. The analysis of exponential beach profiles. J. Coast. Res. 10, 59–69.
Kraus, N.C., Larson, M., 1988. Beach profile change measured in the tank for large waves, 1956–1957 and 1962. Tech. Rep. CERC-88-6, U.S. Army Engineering Waterways Experiment Station, Coastal Engineering Research Center, Vicksburg, MI.
Kroon, A., Masselink, G., 2002. Morphodynamics of intertidal bar morphology on a macrotidal beach under low-energy wave conditions, North Lincolnshire, England. Mar. Geol. 190, 591–608.
Larson, M., 1991. Equilibrium profile of a beach with varying grain size. Coastal Sediments '91, ASCE, pp. 905–919.
Larson, M., Kraus, N.C., Wise, R.A., 1999. Equilibrium beach profiles under breaking and non-breaking waves. Coast. Eng. 36, 59–85.
Levoy, F., Monfort, O., Rousset, H., Larsounneur, C., 1994. Quantification of longshore transport in the surf zone on macrotidal beaches. Proceedings of the 24th International Conference on Coastal Engineering, ASCE, pp. 2282–2296.
Levoy, F., Monfort, O., Larsounneur, C., 2001. Hydrodynamic variability on megatidal beaches, Normandy, France. Cont. Shelf Res. 21, 563–586.
Lippman, T.C., Holman, R.A., 1990. The spatial and temporal variability of sand bar morphology. J. Geophys. Res. 95 (C7), 11575–11590.
Losada, M.A., Medina, R., Vidal, C., Losada, I.J., 1992. Temporal and spatial cross-shore distributions of sediment at 'El Puntal' spit, Santander, Spain. Proceedings of the 23rd International Conference on Coastal Engineering, ASCE, pp. 2251–2264.
Masselink, G., 1993. Simulating the effects of tides on beach morphodynamics. J. Coast. Res. 8, 180–197.
Masselink, G., Short, A.D., 1993. The effect of tide range on beach morphodynamics and morphology: a conceptual beach model. J. Coast. Res. 9, 785–800.
Masselink, G., Hegge, B., 1995. Morphodynamics of meso- and macrotidal beaches: examples from central Queensland, Australia. Mar. Geol. 129, 1–23.
Medina, R., Losada, I., Losada, M.A., Vidal, C., 1995. Variabilidad de los perfiles de playa: forma y distribución granulométrica. Ing. Agua 2, 133–142.
Medina, R., Bernabeu, A.M., Vidal, C., González, E.M., 2000. Relationships between beach morphodynamics and equilibrium profiles. Proceedings of the 27th International Conference on Coastal Engineering, ASCE, pp. 2589–2601.

Moore, B., 1982. Beach Profile Evolution in Response to Changes in Water Level and Wave Height. M.S. Thesis, University of Delaware, Newark, DE.

MOPT, 1992. Recomendaciones para obras marítimas, ROM 0.3-91 Oleaje. Anejo I: Clima Marítimo en el Litoral Español.

Muñoz-Pérez, J.J., Tejedor, L., Medina, R., 1999. Equilibrium beach profile model for reef-protected beaches. J. Coast. Res. 15, 950–957.

Peters, K., Newe, J., Dette, H.-H., 1996. Development of underwater beach profile by monochromatic and random waves. Proceedings of the 26th International Conference on Coastal Engineering, ASCE, pp. 3442–3452.

Saville, T., 1957. Scale effects in two dimensional beach studies. Transactions from the 7th General Meeting of the International Association of Hydraulic Research, vol. 1, pp. A3-1–A3-10.

Short, A.D., 1987. A note on the controls of beach type and changes, with S.E. Australian examples. J. Coast. Res. 3, 387–395.

Short, A.D., 1991. Macro-meso tidal beach morphodynamics – An overview. J. Coast. Res. 7, 417–436.

Sonu, C.F., 1973. Three-dimensional beach changes. J. Geol. 81, 42–64.

Strahler, A.N., 1966. Tidal cycle of changes in an equilibrium beach, Sandy Hook, New Jersey. J. Geol. 74, 247–268.

Sunamura, T., 1989. Sandy beach geomorphology elucidated by laboratory modeling. In: Lakhan, V.C., Trenhail, A.S. (Eds.), Applications in Coastal Engineering. Elsevier, Amsterdam, pp. 159–213.

Vellinga, P., 1983. Predictive computational model for beach and dune erosion during storm surges. Proceedings of the Specialty Conference of Coastal Structures '83, ASCE, pp. 806–819.

Watts, G.M., Dearduff, R.F., 1954. Laboratory study of the effect of tidal action on wave-formed beach profile. U.S. Army Corps of Engineers, Beach Erosion Board Tech. Mem. 52, 21 pp.

Wright, L.D., Short, A.D., 1984. Morphodynamic variability of surf zone and beaches: a synthesis. Mar. Geol. 56, 93–118.

Wright, L.D., Nielsen, P., Short, A.D., Green, M.O., 1982. Morphodynamics of a macrotidal beach. Mar. Geol. 50, 97–128.

Wright, L.D., Short, A.D., Green, M.O., 1985. Short-term changes in the morphodynamic states of beaches and surf zones: an empirical predictive model. Mar. Geol. 62, 339–364.